ARTICLE IN PRESS

+ MODEL

GLOBAL-01200; No of Pages 14

Available online at www.sciencedirect.com

ScienceDirect

ELSEVIER

Global and Planetary Change xx (2006) xxx–xxx

GLOBAL AND PLANETARY CHANGE

www.elsevier.com/locate/gloplacha

Energy balance in the ablation zone during the summer season at the Gran Campo Nevado Ice Cap in the Southern Andes

Christoph Schneider [a,*], Rolf Kilian [b], Michael Glaser [c]

[a] *Geographisches Institut, ~~RW Technische Hochschule Aachen~~, Germany*

[b] *Lehrstuhl für Geologie, FB VI, Universität Trier, Germany*

[c] *Institut für Physische Geographie, Universität Freiburg, Germany*

Abstract

The energy balance and ablation of Glaciar Lengua were investigated during the austral summer of 1999/2000. Glaciar Lengua is located in Patagonia, in the southernmost Andes of Chile (53°S), within an extremely maritime climate. The aim of this study was to gain insight into current energy fluxes at this location and to evaluate how the energy fluxes depend on meteorological variables. From February to April 2000 an automated weather station was operated on Glaciar Lengua. Ablation was measured repeatedly at stakes during the same period. The point energy balance was calculated using the bulk approach formulation. The effective roughness length was adjusted in order to calibrate the model to the measured ablation. It was revealed that sensible heat transfer is the major contribution to the energy balance adding 54% of the energy available for melt. Net radiation contributes only 35% to the overall energy balance. Minor contributors are the latent heat flux (7%) and the heat flux by precipitation (4%). The net radiation shows little variance from day to day. Cross-correlations of the daily mean values of the energy fluxes derived from the energy balance model and meteorological variables reveal that air temperature and wind speed are the key factors controlling the summer energy balance in the ablation area. Melt derived from a multiple regression model based on these two variables correlates with computed melt with a correlation coefficient of 0.92. From the measured ablation, a summer-time degree-day factor of 7.6 mm·°C^{-1} was derived for the ablation area.

Keywords: energy balance; bulk approach; turbulent heat fluxes; ice ablation; degree-day factor; Chile; Patagonia

1. Introduction

The Gran Campo Nevado Ice Cap (GCN) is located in Patagonia at 53°S on the southern part of Península Muñoz Gamero, Chile (Fig. 1). With a surface area of 199.5 km^2, GCN forms the only major ice body between the Southern Patagonia Icefield (SPI) and the Strait of Magellan (Schneider et al., ~~2004~~ this issue). As part of the GCN, Glaciar Lengua was selected as a site for an energy balance study for several reasons: The GCN is located in the west wind zone of the Southern Hemisphere, which is a region of pronounced climate variability also influenced by the El Niño Southern Oscillation phenomena (Turner, 2004; Schneider and Gies, 2004). The GCN is much smaller than the SPI and therefore has a much shorter response time to climate changes. The GCN has shown pronounced glacier recession during the last decades (Schneider et al., ~~2004~~ this issue). Furthermore, there are only few energy balance studies from glaciers of the southernmost

* Corresponding author. Tel.: +49 241 80 96048; fax: +49 241 80 92157.
E-mail address: christoph.schneider@geo.rwth-aachen.de (C. Schneider).

0921-8181/$ - see front matter © 2006 Published by Elsevier B.V.
doi:10.1016/j.gloplacha.2006.11.033

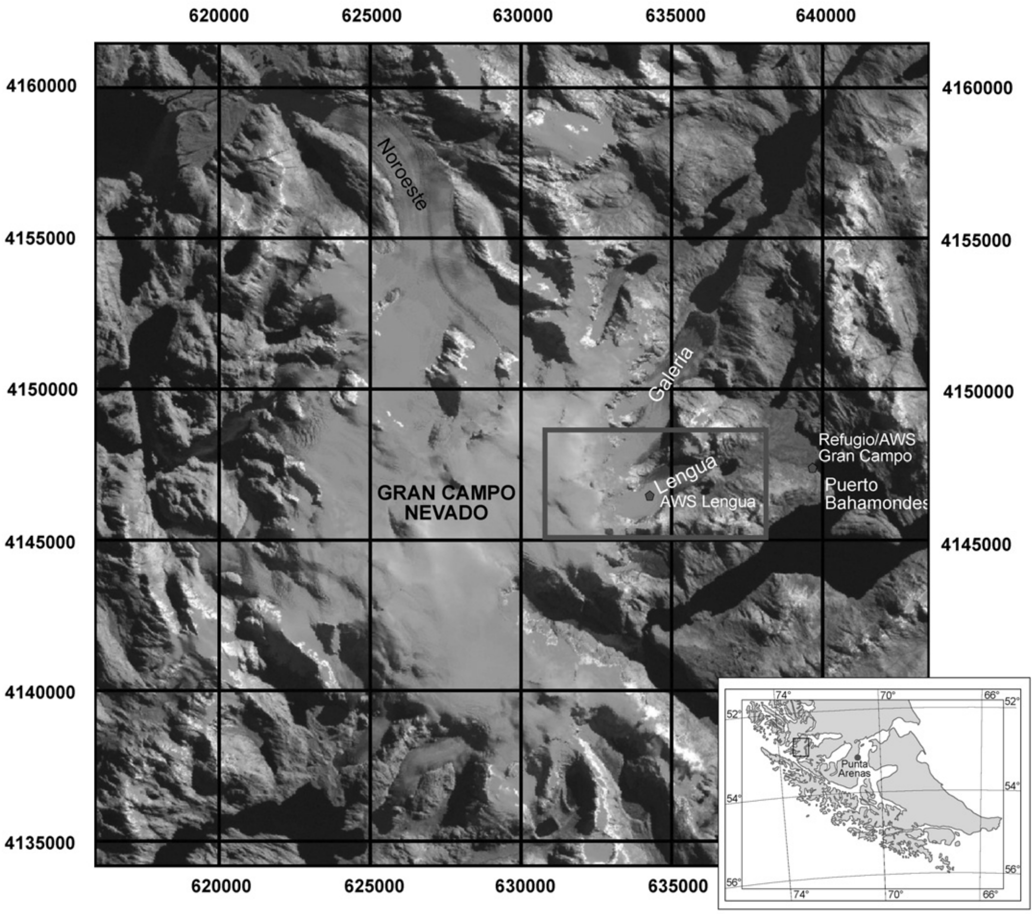

Fig. 1. Satellite image map of Gran Campo Nevado Ice Cap based on a Landsat TM 5 scene from 1986. The rectangle indicates the area covered in Fig. 2.

Andes, and these mostly cover only periods of a few days (Takeuchi et al., 1999). To our knowledge, this study is the first investigation of the energy balance of a glacier in South America south of the SPI.

Generally, climate conditions can be described as extremely windy, moderately cool and very humid (Miller, 1976; Zamora and Santana, 1979). Annual air temperature at the GCN at sea level is +5.7 °C and the mean total annual precipitation at the automated weather station (AWS) at GCN Puerto Bahamondes (for location see Fig. 1) in the east of the ice cap amounts to 6500 mm (Schneider et al., 2003). Daily and seasonal temperature amplitudes are very low due to the vicinity of the Pacific with an amplitude between the warmest and coldest months at AWS GCN Puerto Bahamondes (Fig. 1) of only 7.4 °C (Schneider et al., 2003). Based on the mean lapse rate of 0.65 K·(100 m)$^{-1}$ (Schneider et al., 2003) we estimate a mean annual air temperature of +2.9 °C at the site where an AWS was run at 450 m asl on the glacier in the summer of 1999/2000. At this location the air temperature is almost always above the freezing point throughout the summer season. High precipitation occurs during the whole year with a maximum falling during the austral summer. The increase in precipitation with altitude is considerable. At higher altitudes of the GCN precipitation exceeds 10,000 mm water equivalent (weq) of annual solid precipitation (Schneider et al., 2003).

Glaciar Lengua is the unofficial name of an outlet glacier of the GCN (Fig. 2). The accumulation area of Glaciar Lengua is located on the plateau of the GCN at between 900 and 1700 m asl (Fig. 2). The ablation area ~~of Glaciar Lengua~~ ranges from about 650 to 100 m asl and is connected with the accumulation area by a narrow ice ramp at about 850 m asl. Glaciar Lengua can be characterised as a reconstituted glacier because the ice input to the glacier tongue mainly comes from ice falls. The glacier tongue flows into a proglacial lake that formed during the 20th century (Schneider et al., ~~2004~~ this issue).

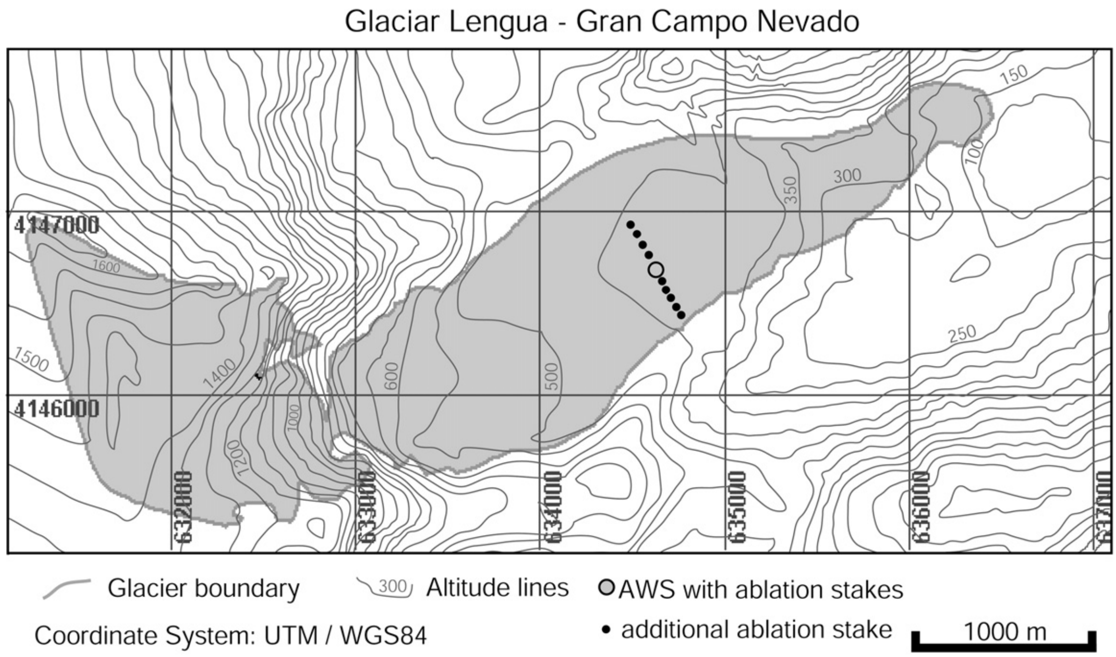

Fig. 2. ~~Ortho-photo m~~ap of Glaciar Lengua and location of AWS on Glaciar Lengua based on aerial photos from 1998. The relationship to the Gran Campo Nevado is shown in Fig. 1.

This paper reports energy balance estimates and the partitioning of the terms of the energy balance measured at an AWS operated in the ablation zone of Glaciar Lengua late in the austral summer of 1999/2000. The equipment was on the glacier for 52 days but ablation measurements, measured at ~~ablation~~ stakes were only ~~available~~ for 45 days. The hypothesis is that the ratio between individual energy balance terms on the glacier tongue reflects the extremely maritime climate conditions. The data ~~is~~ also used for an analysis of cross-correlations between meteorological variables and the terms of the energy balance and the determination of a degree-day factor on Glaciar Lengua for the melt season. The purpose of the approach in this study is to identify the key variables that influence ablation on Glaciar Lengua and to evaluate whether a degree-day model could be run successfully with data from Glaciar Lengua.

Most energy balance studies from different localities indicate that the net radiation generally contributes between 50% and 90% of the energy available for ice melt (Male and Granger, 1981; Hock and Holmgren, 1996; Oerlemans and Klok, 2002; Willis et al., 2002). In maritime climates, as is the case at the GCN, turbulent heat fluxes tend to contribute a larger part of the energy available for melt and sometimes exceed the value of the net radiation (see e.g. Poggi, 1977 and Tab. III in Willis et al., 2002). Takeuchi et al. (1999) compare the partitioning of the terms of the energy balance from the ablation area of 4 outlet glaciers of the Patagonia Icefields. On Soler Glacier sensible heat flux is larger than net radiation and turbulent heat fluxes together make up approximately 70% of the energy balance. On Moreno Glacier, Tyndall Glacier and San Rafael Glacier the net radiation and the turbulent heat fluxes are about equal and sensible heat flux contributes more than 45% in these cases. However, measurements reported by Takeuchi et al. (1999) are derived from short time periods of 15 days (Soler Glacier), 4 days (San Rafael Glacier), 16 days (Moreno Glacier) and 9 days (Tyndall Glacier). Climate conditions similar to those in Patagonia may be found in southern Norway and on the west coast of New Zealand's South Island. In February 1990 Ishikawa et al. (1992) obtained on Franz Josef Glacier (New Zealand) values of 21% for the energy balance from the net radiation, while 80% of the energy available for ice melt came from the turbulent heat fluxes. For Ivory Glacier, New Zealand, Hay and Fitzharris (1988) present values of 52% for the net radiation and 46% for the turbulent heat fluxes during the summer season of 1972/73.

Reviews on the degree-day method are presented e.g. by Braithwaite (1995b), Braithwaite and Zhang (2000),

Please cite this article as: Schneider, C. et al. Energy balance in the ablation zone during the summer season at the Gran Campo Nevado Ice Cap in the Southern Andes. Global and Planetary Change (2006), doi:10.1016/j.gloplacha.2006.11.033

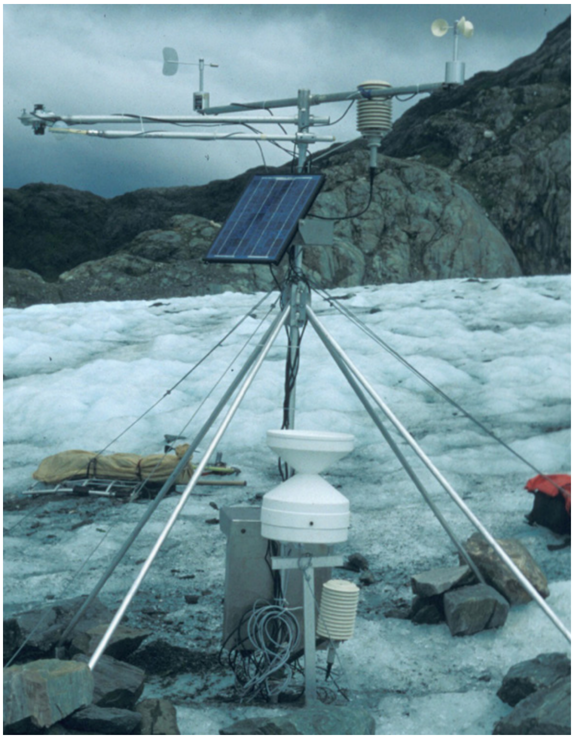

Fig. 3. AWS Glaciar Lengua which was operated from 22 February 2000 until 13 April 2000.

Ohmura (2001) and Hock (2003). Although in most climates the energy for melt is mainly derived from net radiation, many studies show that degree-day models return satisfactory estimates of the ablation. Braithwaite (1981) shows that this is due to the fact that on the basis of daily averages there is much more variance in the course of the sensible heat flux than in the net radiation. Furthermore, the air temperature reflects in a complex manner many processes in the boundary layer. Ohmura (2001), for example, shows that air temperature measured at screen level can be used in many cases as a proxy for atmospheric long-wave radiation. For these reasons, the air temperature is often an appropriate proxy for the energy balance.

2. Data

2.1. Automatic weather station data

The AWS used to acquire meteorological data for the energy balance estimates on Glaciar Lengua was operated from 22 February until 13 April 2000. The AWS carried instrumentation and a data logger supplied by Campbell Scientific Ltd. (UK). Instruments measuring air temperature and air humidity at two levels, precipitation, incoming short-wave radiation, reflected short-wave radiation, net radiation, wind speed and wind direction. All instruments were mounted on a light aluminium tripod resting freely on the ice surface (Fig. 3). The extension arms were fixed by ice screws and piles of loose boulders. The standard measuring height was 2 m above the ground. The air temperature and relative humidity were additionally measured at 0.25 m. Precipitation was measured using an unshielded tipping gauge bucket mounted about 1 m above the surface. Details of all instruments are given in Table 1. Measurements were taken every 10 s and stored as means of 10 min to a storage module. In the case of the precipitation measurement totals of 10 min intervals were stored. Power was supplied by a 10 W solar panel and an internal rechargeable battery.

Maintenance intervals for the AWS ranged from 2 to 5 days depending on weather conditions. On two occasions it was observed that the tripod suffered from an inclination of between 5 and 15° due to surface melting. This can lead to large additional errors especially in short-wave radiation and in precipitation measurements. These errors are discussed in Section 4.2.

Air temperature was measured using unventilated radiation shields which leads to too high air temperature readings during periods with low wind speed and high short-wave radiation because of poor ventilation (Fig. 3) (Hock, 1999; Richardson et al., 1999). The error introduced may be as large as several degrees. Therefore,

Table 1
Instrumentation of automatic weather station

Variable	Instrument	Precision
Air temperature	Combined air humidity temperature probe — ‘HMP-35AC’ (Manufacturer: Vaisala)	<±0.1 °C
Relative humidity	Combined air humidity temperature probe — ‘HMP-35AC’ (Manufacturer: Vaisala)	±2% (RH<90%) ±3% (RH>90%)
Precipitation	Tipping gauge — ‘AGR100’ (Campbell Sci.)	Up to −20%
Wind direction	Wind vane ‘W200P’ (Campbell Sci.)	±2°
Wind speed	Cup anemometer ‘A100R’ (Campbell Sci.)	1% (u<10 m s^{-1}) ±0.1 m s^{-1} (u>10 m s^{-1})
Short-wave radiation	Silicon photo cell ‘SP1110’ (Campbell Sci.)	±5%
Net radiation	Net radiometer ‘Q-6’ (Campbell Sci.)	<15%

Please cite this article as: Schneider, C. et al. Energy balance in the ablation zone during the summer season at the Gran Campo Nevado Ice Cap in the Southern Andes. Global and Planetary Change (2006), doi:10.1016/j.gloplacha.2006.11.033

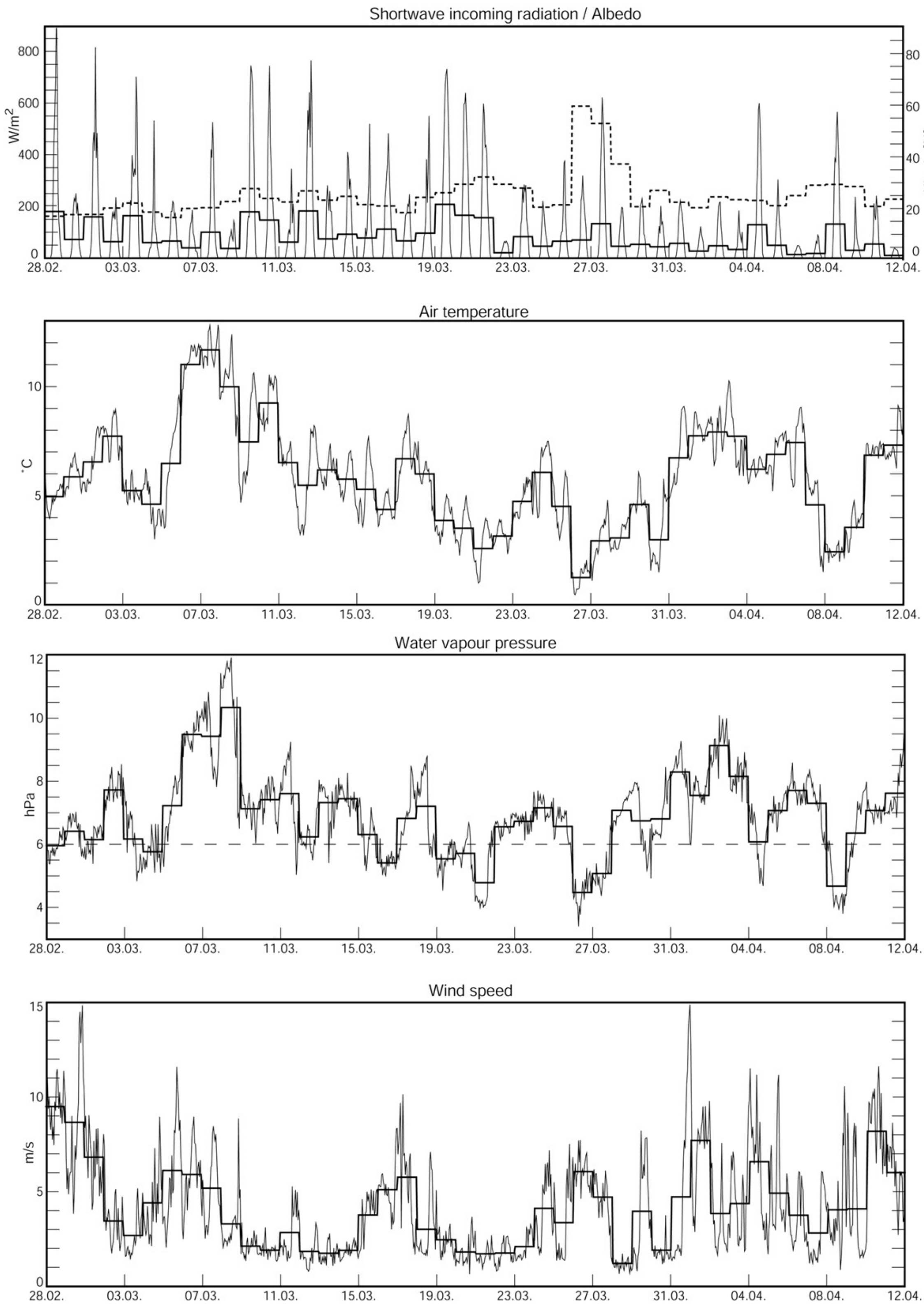

Fig. 4. Hourly and daily means of incoming short-wave radiation, albedo, air temperature, water vapour pressure and wind speed at AWS Glaciar Lengua, 28.02.2000–12.04.2000.

Please cite this article as: Schneider, C. et al. Energy balance in the ablation zone during the summer season at the Gran Campo Nevado Ice Cap in the Southern Andes. Global and Planetary Change (2006), doi:10.1016/j.gloplacha.2006.11.033

measurements of air temperature were corrected according to

$$\Delta T = a \cdot KW \cdot e^{b \cdot u + c} \quad (1)$$

with

ΔT	calculated difference between measured and real air temperature [°C]
a	0.0118, constant, [°C m^2 W^{-2}]
KW	incoming short-wave radiation, [W·m^{-2}]
b	-1.02, constant, [s · m^{-1}]
u	wind speed at screen level, [m · s^{-1}]
c	0.33, constant.

This formulation is in good agreement with correction factors provided by Young Company (U.S.) for radiation shields of this type (Young, 1987). Over snow surfaces with high albedo and during periods with high levels of incoming short-wave radiation the radiation error may be much higher than the mean deviations provided by the manufacturers (Arck and Scherer, 2001). However, since the mean albedo of the glacier surface was only 24% (Fig. 4) the applied correction is considered to be sufficient. At a wind speed of 3.5 m s^{-1} and an incoming short-wave radiation of 600 W·m^{-2} a correction value of 0.28 °C is calculated. Therefore, the correction was not made for wind speeds exceeding 3.5 m·s^{-1}. The remaining error due to short-wave radiation is discussed in Section 4.2.

Data records of main climate variables are shown in Fig. 4. The descriptive statistics are presented in Table 2. The air temperature was positive throughout the measurement period with a mean value of +5.9 °C. Mean daily precipitation was 24 mm.

2.2. Measurement of ablation

Ablation was measured at 9 ablation stakes which were drilled in along a profile perpendicular to the flow line at the position of the AWS with a distance of about 50 m between single stakes (Fig. 2). Close to the AWS 4 additional stakes were drilled in forming a square with sides about 9 m long with the AWS sitting in its centre. Plastic tubes with a diameter of 1 cm and 2.5 m of length were used as ablation stakes. Whereas most stakes sat loosely in the drilled holes a few stakes refroze in their holes or were wedged in the holes due to debris in the bore hole. A piece of metal at the lower end of each stake prevented stakes from eventually coming afloat in the borehole. Ablation was measured each time during maintenance of the AWS resulting in periods ranging from 2 to 5 days. Loose stakes were re-drilled twice so that stakes never sat in the ice with less than 1.5 m of remaining tube length. The mean of the readings from all stakes was taken as the ablation during the time interval. All readings of ice ablation were converted to water equivalent (weq) using a value of the density of ice of 0.9 g cm^{-3}. It is assumed that the different readings at the stakes appropriately cover the variability of ablation in the vicinity of the AWS resulting from locally varying surface slope, exposition and debris cover.

Table 2
Mean, minimum and maximum of measured variables and computed energy balance terms at AWS Glaciar Lengua during 28.02.2000–12.04.2000 based on hourly data

Variable	Min	Mean	Max
Air temperature [°C]	0.5	5.9	12.8
Relative humidity [%]	49	77	98
Water vapour pressure [hPa]	3.4	6.9	11.9
Wind speed [m s^{-1}]	0.6	4.1	14.9
Daily precipitation [mm]	0	24	195
Incoming short-wave radiation [W m^{-2}]	0	85	942
Net radiation [W m^{-2}]	−60	57	650
Sensible heat flux [W m^{-2}]	0	87	478
Latent heat flux [W m^{-2}]	−186	12	222
Energy balance [W m^{-2}]	−134	162	881
Melt water equivalent per hour [mm]	0	1.8	9.5

Ablation ranged from 23 to 68 · 10^{-3} m weq day^{-1} during the 8 measurement intervals between 27 February and 12 April 2000. The mean ablation was 42 · 10^{-3} m weq day^{-1}. Over the entire measurement period the ablation totals 1.88 m weq or 2.09 m of ice. The standard deviations in the measurements of the different time intervals range from 7% to 37% of the measured ablation with a mean of 17% (35 mm). The standard deviation in ablation from all stakes during the complete period is only 4% (82 mm). This reflects similar conditions at the different stakes and it indicates that the ablation measurements can be trusted given that only mean values over all stakes are used.

3. Method

3.1. Energy balance model

The energy balance at the ice surface at any time is given by Paterson (1994)

$$M + S = R + H + E + P \quad (2)$$

with

M	melting of ice	S	change of heat storage in the ice
R	net radiation	H	sensible heat flux
E	latent heat flux	P	heat input by precipitation.

No temperature gradient in the ice and no change in heat storage were observed because the upper layer of ice was almost always at its melting point. Net radiation was directly measured at the AWS. P was calculated from the temperature difference between the precipitation droplets – assumed to be equal to the air temperature ($T(z)$) – and the ice surface (0 °C) and the amount of precipitation per square metre and unit time (N_m) according to

$$P = k \cdot N_\mathrm{m} \cdot T(z) \tag{3}$$

with the heat capacity of water being (k=4.182 · 10^{-3}J · (kg °C)$^{-1}$).

Turbulent heat fluxes were estimated based on the bulk approach (Anderson, 1968; Kuhn, 1979; Braithwaite, 1995a). Based on the temperature and water vapour difference between screen level (z) and the ice surface, the heat transfer can be calculated depending on surface roughness and wind speed. The complete mathematical and physical reasoning of the bulk approach is presented e.g. in Brutsaert (1982), Morris (1991) and Oerlemans (2001). The effect of stable stratification of the boundary layer was included using the bulk Richardson number (Rb) according to Munro (1989) and Braithwaite (1995a). H and E are then given by:

$$H = C_H \rho c_p u(z)(\Theta(z) - \Theta_0)(1 - 5Rb)^2 \quad \text{for } 0<Rb<0.2 \text{ and } H = 0 \text{ for } Rb>0.2 \tag{4}$$

$$E = C_E \frac{\rho L_\mathrm{v} \cdot 0.622 \cdot u(z)}{p}(e(z) - 6.11)(1 - 5Rb)^2 \quad \text{for } 0<Rb<0.2 \text{ and } E = 0 \text{ for} Rb>0.2 \tag{5}$$

with

ρ	density of air
c_p	specific heat of air at constant air pressure (1005 J kg^{-1} K^{-1})
κ	van Karman constant (0.4)
$u(z)$	wind speed at screen level (z)
$\Theta(z)$	potential air temperature at screen level (z)
Θ_0	potential air temperature at the ice surface
$z_{0,u}$	roughness length of momentum
$z_{0,T}$	roughness length of heat
$z_{0,q}$	roughness length of water vapour
L_v	heat of vaporisation (2.514 · 10^6 J kg^{-1}); phase change from water to water vapour and vice versa due to the availability of melt water at the surface when the ice surface has a surface temperature of 0 °C
p	air pressure
$e(z)$	water vapour pressure at screen level (z).

Rb can be calculated using:

$$Rb = \frac{g(\Theta(z) - \Theta_0)(z - z_0)}{\bar{\Theta} u(z)^2} \tag{6}$$

with

$$\bar{\Theta} = \frac{\Theta(z) + \Theta_0}{2}. \tag{7}$$

The bulk heat exchange coefficients (C_H, C_E) for neutral conditions are defined as (e.g. Sharan et al., 2003)

$$C_H = \frac{\kappa^2}{\left[\ln\left(\frac{z}{z_{0,u}}\right)\ln\left(\frac{z}{z_{0,T}}\right)\right]}, \tag{8}$$

$$C_E = \frac{\kappa^2}{\left[\ln\left(\frac{z}{z_{0,u}}\right)\ln\left(\frac{z}{z_{0,q}}\right)\right]}. \tag{9}$$

Eqs. (4) and (5) make use of measurements of humidity, air temperature and wind speed at the surface (z_0) and at height z. At the melting surface the wind speed is zero and the air temperature is 0 °C. The water vapour pressure at the melting surface is 6.11 hPa. The case of unstable stratification of the boundary layer is rarely observed over melting ice surfaces. Therefore, correction for stability is only incorporated for stable situations. All necessary variables in Eqs. (4) and (5) besides the surface roughness lengths are obtained directly from the measurements at the AWS.

In accordance with Braithwaite (1995a) an *effective roughness length* (z_0=z_t=z_q=z_u) was chosen to tune the model to observations such that a linear regression between the measured and modelled melts yielded an optimum fit (least root mean square error) and that the difference between total measured ablation and total calculated ablation was minimised. Effective roughness length obtained by tuning the model in this way must not be confused with theoretically derived or individually measured surface roughness lengths for momentum ($z_{0,u}$) and scaling lengths for temperature ($z_{0,T}$) and humidity ($z_{0,q}$) because theoretically the latter need not be equal (e.g. Moore, 1983; Hock and Holmgren, 1996). Values of effective roughness lengths over snow and ice vary over a wide range from 10^{-6} to 10^{-1} m (Holmgren, 1971; Kuhn, 1979; Moore, 1983; Morris, 1989; Wieringa, 1993; Braun and Schneider, 2000; Oerlemans

Please cite this article as: Schneider, C. et al. Energy balance in the ablation zone during the summer season at the Gran Campo Nevado Ice Cap in the Southern Andes. Global and Planetary Change (2006), doi:10.1016/j.gloplacha.2006.11.033

and Klok, 2002) not only reflecting difficulties in calibrating this parameter but also indicating large differences in observed snow and ice surfaces.

The energy available for melt according to Eq. (2) was transformed into melt water equivalent using the heat of fusion of water of $3.35 \cdot 10^5$ J kg^{-1}. The calculation was performed based on hourly data.

3.2. Cross-correlations, multiple linear regression model and degree-day factor

Cross-correlations between daily means of the terms of the energy balance and meteorological variables were computed using the standard correlation procedure according to Pearson in order to evaluate how ablation depends on the variables. The significance of the correlations was tested employing a two-tailed Student's *t*-test.

Based on the findings of the cross-correlations a multiple linear regression model (MLRM, Eq. (10)) was calculated using daily (i) means of temperature T_i and wind speed u_i to predict daily means of the ablation (A_i):

$$A = \sum_i A_i = \sum_i (c_0 + c_T \cdot T_i + c_u u_i). \qquad (10)$$

The coefficients of the MLRM (c_0, c_T, c_u) were determined using a two dimensional least root mean square fit of T_i and u_i against A_i.

As melt usually occurs only during time periods with positive air temperatures the simplification of the linear regression model to T_i as the only predicting variable with $c_0=0$ yields a degree-day model given by (e.g. Hock, 2003)

$$A = \sum_i A_i = c \sum_i T_i \text{ if } T_i > 0\ ^\circ\text{C and} \qquad (11)$$

$$A_i = 0 \text{ if } T_i \leq 0.$$

In this case the degree-day factor (c) can be obtained by dividing the total measured ablation (A) by the temperature sum of all days with $T_i>0$ and the total number of days. This procedure was applied to the data in this study.

4. Results and discussion

4.1. Energy balance modelling

Optimum agreement between modelled and measured ablation rates was achieved using a value for the effective roughness length of $z_0=3.3 \cdot 10^{-3}$ m. This value is rather large compared with the range of values reported in earlier studies (e.g. Kuhn, 1979; Morris, 1989; Wieringa, 1993). The bulk heat exchange coefficient (C_H) then is calculated to $C_H=3.9 \cdot 10^{-3}$ using a measurement height (z) of 2.0 m. Consequently, this value is large in comparison to values obtained by, for example, Hogg et al. (1982, $C_H=1.3 \cdot 10^{-3}$), Oerlemans (2000, $C_H=1.2 \cdot 10^{-3}$) and Oerlemans and Klok (2002, $C_H=1.55 \cdot 10^{-3}$). However, the values seem to be reasonable in view of the rugged glacier surface of the ablation area of Glaciar Lengua. Values for C_H and z_0 also depend on the applied parameterisation scheme of atmospheric stability and on assumptions regarding the similarity of the roughness lengths of momentum, energy and moisture. C_H also depends on the measuring height. Therefore, the values obtained by different authors cannot easily be compared with each other.

Modelled and measured ablation rates are compared with each other in Fig. 5. The correlation coefficient of $r=0.98$ is very high. However, it is based only on eight measurement intervals ranging from 98 to 196 h. Descriptive statistics of the computed terms of the energy balance are presented in Table 2. The mean energy available for melt is +162 W m^{-2}. The partitioning of the terms of the energy balance at Glaciar Lengua is similar to the results obtained in other highly maritime environments reported in the Introduction. Accordingly, the cool, windy and humid regional climate of south-west Patagonia is considered to be responsible for the high contribution (54%) of the sensible heat flux to the ablation at Glaciar Lengua. High overall cloud cover hampers radiative cooling of the boundary layer air mass keeping sensible heat flux high even during night-time. During the investigation period the mean air temperature

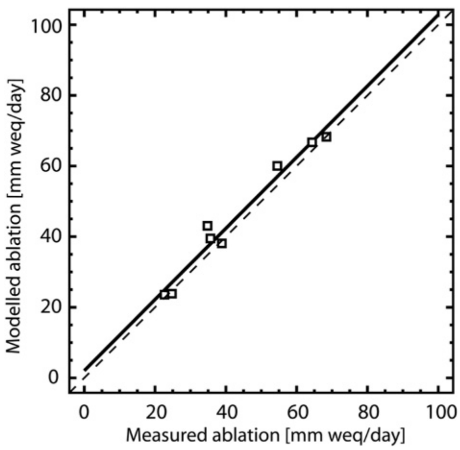

Fig. 5. Measured and modelled ablation in the ablation area of Glaciar Lengua at 450 m asl during eight periods between 28.02.2000 and 12.04.2000. The stippled line denotes the perfect one-to-one fit. The solid line shows the fitted linear regression line.

Please cite this article as: Schneider, C. et al. Energy balance in the ablation zone during the summer season at the Gran Campo Nevado Ice Cap in the Southern Andes. Global and Planetary Change (2006), doi:10.1016/j.gloplacha.2006.11.033

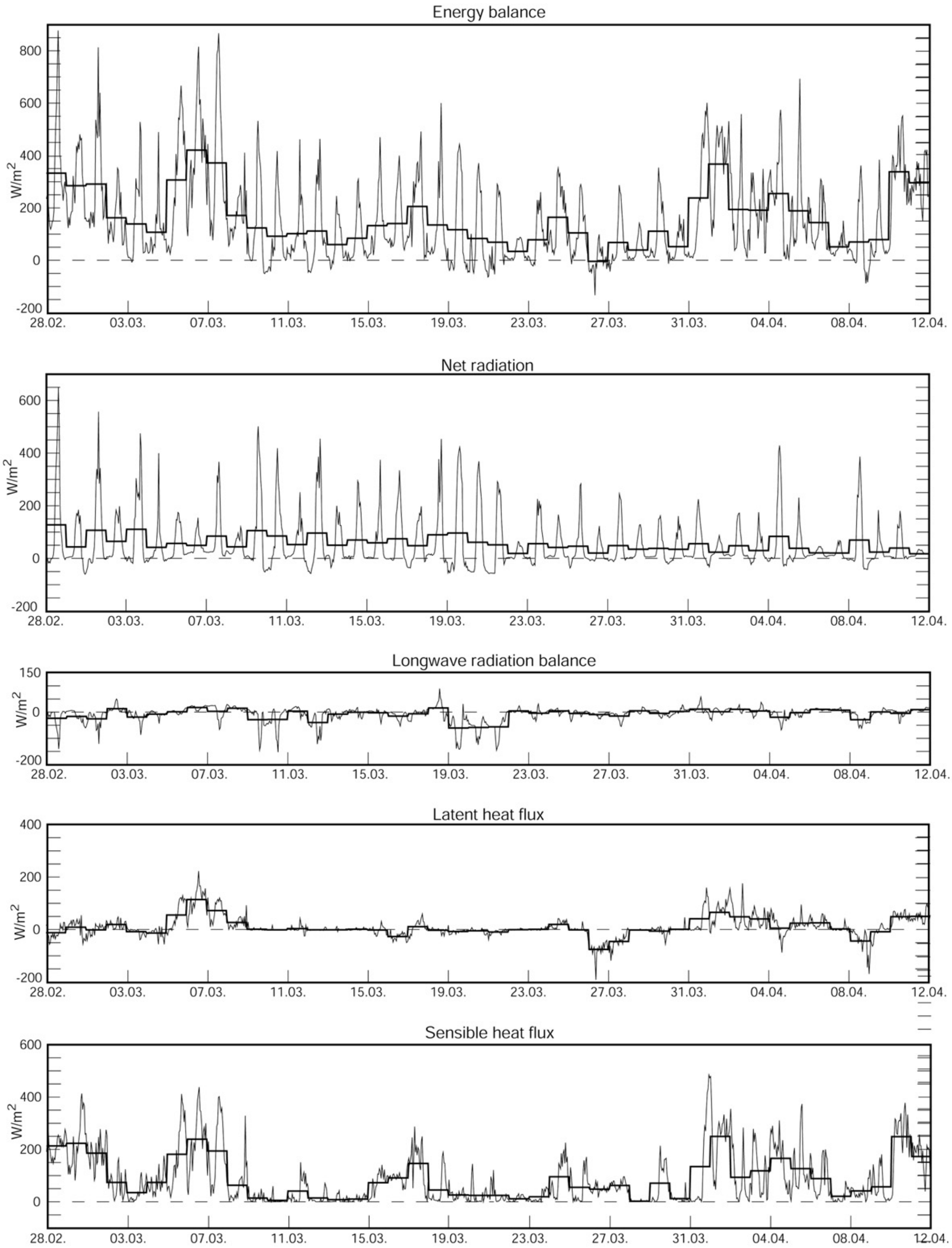

Fig. 6. Hourly and daily means of the terms of the energy balance at AWS Glaciar Lengua, 28.02.2000–12.04.2000. The energy balance (top) is equivalent to the energy available for melt.

Please cite this article as: Schneider, C. et al. Energy balance in the ablation zone during the summer season at the Gran Campo Nevado Ice Cap in the Southern Andes. Global and Planetary Change (2006), doi:10.1016/j.gloplacha.2006.11.033

at the AWS was always positive with a mean of +5.9 °C (Table 2). This constantly produced a strong temperature gradient towards the ice surface even at night-time. In combination with the high mean wind speed (4.1 m s^{-1}) and the rugged ice surface this led to the high mean value of the sensible heat flux of +86 W m^{-2}. In most studies the net radiation is the largest contributing factor to the summer time energy balance over melting glacier surfaces (see Introduction). In the case of Glaciar Lengua it is only the second important contributing factor with +57 W m^{-2} (35%). The mean water vapour pressure during the period of investigation (6.9 hPa, Table 2) is larger than the saturation water vapour pressure at the melting point (6.11 hPa) indicating a small gradient of humidity towards the ice surface. Therefore, latent heat flux contributes a small portion to the energy balance with +12 W m^{-2} (7%) which implies that on average condensation on the surface can be observed. The surplus of energy resulting from rainfall adds +6 W m^{-2} (4%) to the total energy balance.

In Fig. 6 hourly data and daily means of the different terms of the energy balance are presented. The balance of long-wave radiation fluxes does not significantly vary in time due to constant ice surface temperature and the rather small variation of atmospheric long-wave radiation. Therefore, the daily course of the net radiation and its variability over a longer term are mainly determined by incoming short-wave radiation. In consequence, hourly values of the radiation budget and the energy balance reflect the daily cycle of the short-wave radiation. The mean albedo measured at the AWS during the measurement period was 24%, which is in agreement with published values for partially debris covered glacier ice (Cutler and Munro, 1996; Gao and Liu, 2001). The largest values of the energy balance coincide with the maximum values of incoming solar radiation around noon. However, the daily means presented in Fig. 6 show that the variability of the radiation budget on a daily basis is small compared with the variance of the turbulent heat fluxes. Due to the small or even negative net radiation during the night the net radiation is on average smaller than the average of the sensible heat flux.

Glaciar Lengua reaches down to low altitudes and is situated in a very maritime climate. Both facts generally indicate that the relative contribution of the sensible heat flux to the energy balance is comparatively large (Braithwaite, 1981). Since the sensible heat flux depends directly on the air temperature, it can be hypothesised that simple methods based on air temperature records can be applied to estimate ablation on Glaciar Lengua.

During some periods, especially during the night, small negative values of the energy balance were obtained. This indicates some change in internal heat storage, especially re-freezing of water at the surface. Consequently, positive energy balance during the following time intervals must compensate for the negative heat storage before any further melt can occur. However, since there are only short intervals with negative energy balance and the absolute negative values are small, the error introduced from this is assumed to be negligible.

4.2. Error analysis of the energy balance model

Since the energy balance is closed by tuning the effective roughness length such that the turbulent heat fluxes, the precipitation heat flux and the net radiation match the measured melt it is reasonable to discuss possible sources of error in the three measurements and to calculate the possible error of the turbulent heat fluxes by the law of error propagation of Gauss on the basis of the mean values found in this study.

In addition to the standard error of the net radiation instrument of ±15% provided by the manufacturer, large errors may occur when the tripod of the AWS was tilted due to surface melting. This occurred during two intervals (see Section 2.1). However, it is unclear how many hours were affected within these two periods. There are different possibilities how this error may affect the measurements. For example, if the upper side of the instrument receives less short-wave radiation and the side facing downwards receives more short-wave radiation, this mostly leads to an underestimation of the short-wave net radiation. This effect can only occur during the day and leads to large errors mainly under clear sky conditions. In part, this error is compensated by the long-wave radiation, which in most cases will be slightly overestimated when the instrument is not levelled correctly. For a conservative estimate of the possible error we assume that a very large error due to the tilt of the mast of 50% occurred twice for periods of two days within the complete period of 45 days. This translates into an additional mean error of 4.5% over the complete period. Given that smaller tilt angles might have been present during longer intervals (additional 5%) we assume that, overall, the additional error from this source does not exceed ±10%. However, the error of some single measurements could have been much larger than this value. In consequence, we finally have a total mean error for the net radiation measurement (ΔR) of ±25% or ±14.2 W m^{-2}.

Precipitation measurements are very prone to error due to wind-induced drift of droplets and evaporation

Please cite this article as: Schneider, C. et al. Energy balance in the ablation zone during the summer season at the Gran Campo Nevado Ice Cap in the Southern Andes. Global and Planetary Change (2006), doi:10.1016/j.gloplacha.2006.11.033

from the collecting bucket (Sevruk, 1982; Yang et al., 1999). Tilt of the tripod would increase these errors that are primarily due to wind drift. Therefore, an error of 50% of the precipitation measurement (ΔN) must be taken into account. The heat flux by precipitation itself is of minor importance (see Section 4.1). Therefore, even the large overall error of 50% would alter the energy balance only by less than ±3.5 W m^{-2} including an uncertainty of ±0.5 K of the temperature of the precipitation water.

The mean standard deviation of the readings from the ablation stakes (±17%, see Section 2.2) was taken as an estimate of the error of measured ablation (ΔM=±27.5 W m^{-2}).

Based on the mean values of the terms of the energy balance according to Eq. (2) and the error propagation derived from Eq. (2), the mean error of the turbulent heat fluxes (ΔHE) can be calculated by

$$\Delta HE = \sqrt{(\Delta R^2) + (\Delta M^2) + (\Delta N^2)} \qquad (12)$$

to ±31.1 W m^{-2} or 31.4% of the mean sum of the turbulent heat fluxes.

The error of the turbulent heat exchange coefficient C_H must be larger than ΔHE because of possible errors of the measurements of wind speed, relative humidity and air temperature.

The error of the temperature measurement due to radiative heating of the sensor within the unventilated radiation shield has been corrected according to Eq. (1). Overall, the high mean wind speed (4.1 m s^{-1}) and the rather low mean incoming short-wave radiation of 85 W m^{-2} and the low albedo of only 24% suggest that radiative heating of the temperature and humidity probe was of minor importance. Furthermore, the combination of short-wave radiation exceeding 200 W m^{-2} and a wind speed of less than 3.5 m s^{-1} only occurred during 8% of the time. In order to account for any residual radiative error and calibration error a large error of ±0.5 K was assumed for further analysis. This value by far exceeds the standard error provided by the manufacturer (Table 1). The mean error of the wind speed was taken as ±0.2 m s^{-1} and a value of ±5% was chosen as the mean error for relative humidity. Under the assumption of a fixed value for C_H=C_E=3.9 · 10^{-3} (see Section 4.1) a mean error of the latent heat flux (ΔE) of ±11.4 W m^{-2} (±95%) was obtained. The maximum error of the sensible heat flux (ΔH) derived by error propagation of the other terms of the energy balance (ΔHE) and ΔE is then calculated to be ±33.1 W m^{-2} or 38% of the mean sensible heat flux. Based on this calculation we obtain a probable interval for C_H of 3.9 · 10^{-3} ± 1.5 · 10^{-3}. The combined error of all terms of the energy balance derived from error propagation results in an error estimate for the mean calculated melt of 162 ± 38 W m^{-2}.

4.3. Cross-correlation, multiple linear regression and degree-day factor

The correlation coefficients presented in Table 3 show the quality of the linear relationships between the daily means of the terms of the energy balance and different meteorological variables. Correlations that are significant above the 99% level are typed in bold numbers. Surprisingly, there are no significant correlations between ablation and net radiation or incoming short-wave radiation. The main reason for this is that both radiation variables show a strong daily cycle, but exhibit low variability from day to day as can be seen in Fig. 6 (see also Braithwaite, 1981). Furthermore, both radiation variables have no strong correlation with any other variable besides with each other and with relative humidity. Short-wave radiation and relative humidity are negatively correlated reflecting the fact that high relative humidity is linked to enhanced cloud cover. This in turn is the reason why the short-wave radiation and the latent heat flux are also negatively correlated.

Table 3
Cross-correlation of daily averages of ablation and the terms of the energy balance and selected meteorological variables derived from AWS on Glaciar Lengua run from 28.02.2000 to 12.04.2000. Correlations significant at the 99% level are given in bold numbers

	Calc. melt	Net rad.	Sens. hf.	Lat. hf.	Air temp.	S.-w. rad.	Wind sp.	Rel. hum.
Calculated melt		0.14	0.94	0.74	0.64	−0.08	0.78	−0.25
Net radiation	0.14		−0.08	−0.19	0.07	0.88	−0.06	−0.47
Sens. heat flux	0.94	−0.08		0.61	0.47	−0.24	0.92	−0.25
Latent heat flux	0.74	−0.19	0.61		0.78	−0.42	0.28	0.24
Temperature	0.64	0.07	0.47	0.78		−0.23	0.22	0.00
Short-wave rad.	−0.08	0.88	−0.24	−0.42	−0.23		−0.15	−0.60
Wind speed	0.78	−0.06	0.92	0.28	0.22	−0.15		−0.37
Rel. humidity	−0.25	−0.47	−0.25	0.24	0.00	−0.60	−0.37	

Please cite this article as: Schneider, C. et al. Energy balance in the ablation zone during the summer season at the Gran Campo Nevado Ice Cap in the Southern Andes. Global and Planetary Change (2006), doi:10.1016/j.gloplacha.2006.11.033

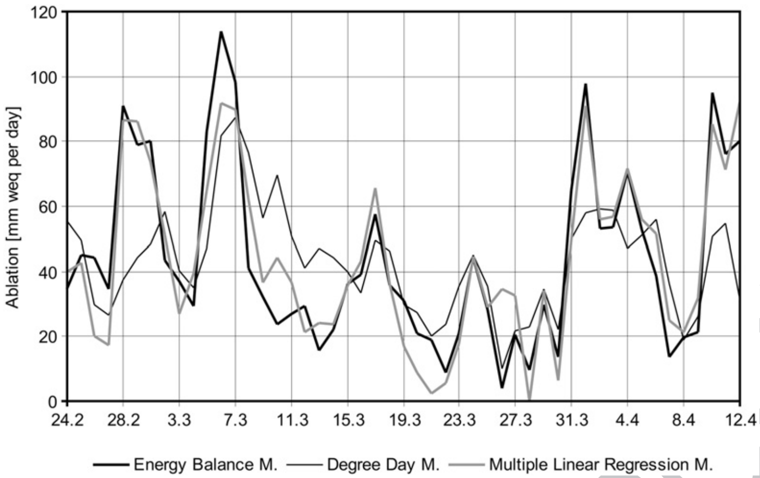

Fig. 7. Daily means of ablation on Glaciar Lengua at 450 m asl for the period 24.02.2000–12.04.2000 according to the energy balance model, the degree-day model and a multiple linear regression model, using air temperature and wind speed as predicting variables.

Ablation depends strongly on wind speed (r=+0.78) and air temperature (r=+0.64). The highest correlation between ablation and any other variable is found with the sensible heat flux (r=+0.94). Additionally, ablation and latent heat flux (r=+0.74) are highly correlated. Both turbulent fluxes show high correlations with wind speed. This is due to the fact that they directly depend on $u(z)$ as can be seen from Eqs. (4) and (5). Air temperature does show considerable correlation with both turbulent heat fluxes (r_H=0.47, r_E=0.78) but only moderate correlation with wind speed (r=0.22). The high correlation between wind speed and the energy balance is probably based on a constantly large positive temperature gradient towards the ice surface during the measurement period. During colder periods (e.g. other seasons of the year) the temperature gradient may be small and frequently alternate between positive and negative values. It is very likely that during such periods there is no good correlation between the wind speed and the energy balance.

Daily data shown in Fig. 6 and the cross-correlations presented in Table 3 indicate that the MLRM with air temperature and wind speed as predictors can be used to obtain statistically derived estimates of ablation in the ablation zone of Glaciar Lengua in summer. The multiple correlation coefficient between these two predictors and the physically based energy balance record is r_{m}=0.92, which implies that the statistical model can explain 85% of the variance that is observed in the energy balance model. According to Table 3 the degree-day model solely based on air temperature correlates with the energy balance model with r=0.64. Consequently, 41% of the variance which appears in the daily means of the energy balance model is picked up by the degree-day model. Fig. 7 illustrates the good agreement between the energy balance model and the MLRM. It can be seen that the record of daily ablation derived from the degree-day model differs significantly from the values based on the energy balance model. However, it can be deduced that the general pattern is similarly depicted in both records.

The average degree-day factor over the period from 27 February until 12 April 2000 is 7.6 mm (°C·day)$^{-1}$. The surface was mostly bare ice although a summer snowfall covered the area for 2 to 3 days from 26 March until 28 March. Degree-day factors observed by other authors from different locations around the world range from 5.4 to 20.0 mm (°C day)$^{-1}$ (Braithwaite and Olesen, 1989; Laumann and Reeh, 1993; Boggild et al., 1994; Braithwaite, 1995b; Jóhannesson et al., 1995; Konzelmann and Braithwaite, 1995; Hock, 1999, 2003). The median of all presented values is 7.0 mm (°C·day)$^{-1}$. From all values 80% range between 6.0 and 8.5 mm (°C·day)$^{-1}$. The degree-day factor for bare glacier ice in the ablation zone of Glaciar Lengua falls within the given range of values.

5. Conclusion

The maritime climate at the GCN and the fact that glacier tongues reach down almost to sea level lead to a large percentage of the sensible heat flux relative to the total energy being available for melt in the ablation zone during summer. At Glaciar Lengua the sensible heat flux contributed 54±20% or 86±~~18~~ W·m^{-2} to the energy balance in the ablation area of Glaciar Lengua in the summer of 1999/2000. Because of the large sensible heat

Please cite this article as: Schneider, C. et al. Energy balance in the ablation zone during the summer season at the Gran Campo Nevado Ice Cap in the Southern Andes. Global and Planetary Change (2006), doi:10.1016/j.gloplacha.2006.11.033

flux it is probably possible to run a degree-day model for longer periods, using air temperature data from an AWS operating in the vicinity of the glacier at Puerto Bahamondes (Schneider et al., 2003 and Fig. 1). The degree-day factor obtained for ice melt is 7.6 mm (day °C)$^{-1}$. With an MLRM based on air temperature and wind speed a much better correlation with the energy balance model based on daily means can be achieved than with the degree-day model. However, the MLRM is not suitable for a long-term estimation of ablation because there is no evidence that the linear relation between ablation and wind speed would be valid for other seasons with mean air temperature around or below the melting point. However, at Glaciar Lengua wind speed is a key variable during the summer, which explains much of the observed variance in ablation on a day-to-day time scale.

Acknowledgements

The authors wish to thank Matthias Faller, Tobias Fischbach, Miriam Hohner, Johannes Koch and Markus Stickling for their assistance in the field. Comments on an earlier version of the manuscript by Regine Hock and an anonymous reviewer are gratefully acknowledged. This study was undertaken funded by grant No. Schn-680 1/1 and Ki-456/6-1 of the German Research ~~Society~~ (Deutsche Forschungsgemeinschaft: DFG).

References

Anderson, E.A., 1968. Development and testing of snow pack energy balance equations. Water Resources Research 4, 19–37.

Arck, M., Scherer, D., 2001. A physically based method for correcting temperature data measured by naturally ventilated sensors over snow. Journal of Glaciology 47, 665–670.

Boggild, C.E., Reeh, N., Oerter, H., 1994. Modelling ablation and mass-balance sensitivity to climate change of Storstrommen, Northeast Greenland. Global and Planetary Change 9, 79–90.

Braithwaite, R.J., 1981. On glacier energy balance, ablation, and air temperature. Journal of Glaciology 27, 381–391.

Braithwaite, R.J., 1995a. Aerodynamic stability and turbulent sensible-heat flux over a melting ice surface, the Greenland ice sheet. Journal of Glaciology 41, 562–571.

Braithwaite, R.J., 1995b. Positive degree-day factors for ablation on the Greenland ice sheet studied by energy-balance modelling. Journal of Glaciology 41, 153–160.

Braithwaite, R.J., Olesen, O.B., 1989. Calculation of glacier ablation from air temperature, West Greenland. In: Oerlemans, J. (Ed.), Glacier Fluctuations and Climatic Change. Kluwer Academic Publishers, pp. 219–233.

Braithwaite, R.J., Zhang, Y., 2000. Sensitivity of mass balance of five Swiss glaciers to temperature changes assessed by tuning a degree-day model. Journal of Glaciology 46, 7–14.

Braun, M., Schneider, C., 2000. Characteristics of summer energy balance on the west coast of the Antarctic Peninsula. Annals of Glaciology 31, 179–183.

Brutsaert, W., 1982. Evaporation into the Atmosphere: Theory, History, Applications. Environmental Fluid Mechanics, Dordrecht.

Cutler, P.M., Munro, D.S., 1996. Visible and near-infrared reflectivity during the ablation period on Peyto Glacier, Alberta, Canada. Journal of Glaciology 42, 333–340.

Gao, J., Liu, Y., 2001. Applications of remote sensing, GIS and GPS in glaciology: a review. Progress in Physical Geography 25, 520–540.

Hay, J.E., Fitzharris, B.B., 1988. A comparison of the energy-balance and bulk-aerodynamic approaches for estimating glacier melt. Journal of Glaciology 34, 145–153.

Hock, R., 1999. A distributed temperature-index ice- and snowmelt model including potential direct solar radiation. Journal of Glaciology 45, 101–112.

Hock, R., 2003. Temperature index melt modelling in mountain areas. Journal of Hydrology 282, 104–115.

Hock, R., Holmgren, B., 1996. Some aspects of energy balance and ablation of Storglaciären, Northern Sweden. Geografiska Annaler 78 A, 121–131.

Hogg, I.G.G., Paren, J.G., Timmis, R.J., 1982. Summer heat and ice balances on Hodges Glacier, South Georgia, Falkland Islands Dependencies. Journal of Glaciology 28, 221–238.

Holmgren, B., 1971. Climate and energy exchange on a sub-polar ice cap in summer. Meddelande, vol. 108. Meteorologiska Institutionen Uppsala Universitet, Uppsala.

Ishikawa, N., Owens, I.F., Sturman, A.P., 1992. Heat balance characteristics during fine periods on the lower parts of the Franz Josef Glacier, south Westland, New Zealand. International Journal of Climatology 12, 397–410.

Jóhannesson, T., Sigurdsson, O., Laumann, T., Kennett, M., 1995. Degree-day glacier mass-balance modelling with applications to glaciers in Iceland, Norway and Greenland. Journal of Glaciology 41, 345–358.

Konzelmann, T., Braithwaite, R.J., 1995. Variations of ablation, albedo and energy balance at the margin of the Greenland ice sheet, Kronprins Christian Land, eastern north Greenland. Journal of Glaciology 41, 174–182.

Kuhn, M., 1979. On the computation of heat transfer coefficients from energy-balance gradients on a glacier. Journal of Glaciology 22, 263–272.

Laumann, T., Reeh, N., 1993. Sensitivity to climate change of the mass balance of glaciers in southern Norway. Journal of Glaciology 39, 656–665.

Male, D.H., Granger, R.J., 1981. Snow surface energy exchange. Water Resources Research 17, 609–627.

Miller, A., 1976. The climate of Chile. In: Schwerdtfeger, W. (Ed.), Climates of Central and South America. World Survey of Climatology, vol. 12. Elsevier, Amsterdam, pp. 113–146.

Moore, R.D., 1983. On the use of bulk aerodynamic formulae over melting snow. Nordic Hydrology 14, 193–206.

Morris, E.M., 1989. Turbulent transfer over snow and ice. Journal of Hydrology 105, 205–223.

Morris, E.M., 1991. Parameterization of turbulent transfers between glaciers and the atmosphere. Glaciers-Ocean-Atmosphere Interactions (Proceedings of the International Symposium held at St. Petersburg, Sept. 1990). IAHS Publ., vol. 208, pp. 543–549.

Munro, D.S., 1989. Surface roughness and bulk heat transfer on a glacier: comparison with eddy correlation. Journal of Glaciology 35, 343–348.

Oerlemans, J., 2000. Analysis of a 3 year meteorological record from the ablation zone of Morteratschgletscher, Switzerland: energy and mass balance. Journal of Glaciology 46, 571–579.

Please cite this article as: Schneider, C. et al. Energy balance in the ablation zone during the summer season at the Gran Campo Nevado Ice Cap in the Southern Andes. Global and Planetary Change (2006), doi:10.1016/j.gloplacha.2006.11.033

Oerlemans, J., 2001. Glaciers and climate change. Balkema Publishers, Lisse, Tokyo.

Oerlemans, J., Klok, E.J., 2002. Energy balance of a glacier surface: analysis of automatic weather station data from the Morteratschgletscher, Switzerland. Arctic, Antarctic, and Alpine Research 34, 477–485.

Ohmura, A., 2001. Physical basis for the temperature-based melt-index method. Journal of Applied Meteorology 40, 753–761.

Paterson, W.S.B., 1994. The Physics of Glaciers, 3rd edition. Elsevier, Kidlington, New York.

Poggi, A., 1977. Heat balance in the ablation area of the Ampere Glacier (Kerguelen Islands). Journal of Applied Meteorology 16, 48–55.

Richardson, S.J., Brock, F.V., Semmer, S.R., Jirak, C., 1999. Minimising errors associated with multiplate radiation shields. Journal of Atmospheric and Oceanic Technology 16, 1862–1872.

Schneider, C., Gies, D., 2004. Effects of El Niño-Southern Oscillation on Southernmost South America precipitation at 53°S revealed from NCEP/NCAR reanalyses and weather station data. International Journal of Climatology 24, 1057–1076.

Schneider, C., Glaser, M., Kilian, R., Santana, A., Butorovic, N., Casassa, G., 2003. Weather observations across the Southern Andes at 53°S. Physical Geography 24, 97–119.

Schneider, C., Schnirch, M., Acuña, C., Casassa, G., Kilian, R., 2004. Glacier inventory of the Gran Campo Nevado Ice Cap in the Southern Andes and glacier changes observed during recent decades. Global and Planetary Change, this issue.

Sevruk, B., 1982. Methods of correction for systematic error in point precipitation measurement for operational use. Operational Hydrology Report, vol. 21. WMO, Geneva.

Sharan, M., Rama Krishna, T.V.B.P.S., Aditi, 2003. Surface-layer characteristics in the stable boundary layer with strong and weak winds. Boundary-Layer Meteorology 108, 257–288.

Takeuchi, Y., Naruse, R., Satow, K., Ishikawa, N., 1999. Comparison of heat balance characteristics at five glaciers in the Southern Hemisphere. Global and Planetary Change 22, 201–208.

Turner, J., 2004. El Niño-Southern Oscillation and the Antarctic. International Journal of Climatology 24, 1–31.

Wieringa, J., 1993. Representative roughness parameters for homogeneous terrain. Boundary-Layer Meteorology 63, 323–363.

Willis, I.C., Arnold, N.S., Brock, B.W., 2002. Effect of snow pack removal on energy balance, melt and runoff in a small supraglacial catchment. Hydrological Processes 16, 2721–2749.

Yang, D., Metcalfe, B.E., Goodison, J.R., Louie, P., Leavesley, G., Emerson, D., Hanson, C.L., Golubev, V.S., Elomaa, E., Gunther, T., Pangburn, T., Kang, E., Milkovic, J., 1999. Quantification of precipitation measurement discontinuity induced by wind shields on national gauges. Water Resources Research 35, 491–508.

Young (Company), 1987. Product Information to Radiation Shield 'Model 41002'.

Zamora, E., Santana, A., 1979. Characteristicas climaticas de la costa occidental de la Patagonia entre las latitudes 46°40′ y 56°30′. Anales del Instituto de la Patagonia. Serie Ciencias Naturales 10, 109–143.

Please cite this article as: Schneider, C. et al. Energy balance in the ablation zone during the summer season at the Gran Campo Nevado Ice Cap in the Southern Andes. Global and Planetary Change (2006), doi:10.1016/j.gloplacha.2006.11.033